Proceedings of the 35th European Safety and Reliability & the 33rd Society for Risk Analysis Europe Conference
Edited by Eirik Bjorheim Abrahamsen, Terje Aven, Frederic Bouder, Roger Flage, Marja Ylönen
 Published by Research Publishing, Singapore.
doi: 10.3850/978-981-94-3281-3_ESREL-SRA-E2025-P7274-cd

Modeling of Accidental Liquid Hydrogen Spills and Rainout

Davide Rescigno

Department of Mechanical and Industrial Engineering, Norwegian University of Science and Technology, Richard Birkelands vei 2B, 7034 Trondheim, Norway. E-mail: davide.rescigno@ntnu.no

Alessandro Campari

Department of Mechanical and Industrial Engineering, Norwegian University of Science and Technology, Richard Birkelands vei 2B, 7034 Trondheim, Norway. E-mail: alessandro.campari@ntnu.no

Alexandros Venetsanos

Environmental Research Laboratory, National Centre for Scientific Research Demokritos (NCSRD), Aghia Paraskevi, Attikis, 15310 Athens, Greece. E-mail: venets@ipta.demokritos.gr

Federico Ustolin

Department of Mechanical and Industrial Engineering, Norwegian University of Science and Technology, Richard Birkelands vei 2B, 7034 Trondheim, Norway. E-mail: federico.ustolin@ntnu.no

Liquid hydrogen (LH_2) is a clean energy carrier that is gaining traction for its versatility. Nevertheless, its use may lead to significant risks due to its low storage temperature, low boiling point, rapid vaporization, and high flammability. In the event of a loss of containment, if a portion of the LH_2 does not fully vaporize and reaches the ground, the rainout phenomenon occurs. If the release is continuous, a pool of LH_2 might be generated, raising the risk of delayed ignition, which may lead to large-scale fires or explosions. Thus, this study aims to understand the behavior of such cryogenic releases to mitigate potential risks. The simulations of LH_2 releases involve the analysis of key factors such as the quality of the fluid, operating pressure of the tank, and jet velocity. This study adopts an integral model to predict the diameter of the LH_2 droplets and their vaporization rate, the rainout, and the potential formation of an LH_2 pool. The simulations help assess worst-case scenarios and determine the LH_2 concentration profiles on the ground. The integral model allows for a preliminary evaluation of real-world release scenarios in hydrogen storage and transport.

Keywords: Hydrogen safety, liquid hydrogen storage, liquid hydrogen spillages, rainout, pool formation, integral model.

1. Introduction

Global warming is a critical problem that calls for immediate solutions. To keep the global temperature increase within 1.5 K, the use of carbon-neutral fuels and carbon capture and storage technologies should be encouraged (Semieniuk et al. 2021). Hydrogen is a clean energy vector that, thanks to its lower heating value of 120 MJ/kg (Juangsa et al. 2018), may be considered one of the major players in world decarbonization. However, hydrogen, especially in its liquid form, poses several challenges. Firstly, liquid hydrogen needs to be stored at cryogenic temperatures, necessitating advanced insulation or active cooling systems to keep its temperature below the evaporation point (Aziz 2021). Secondly, there are various safety issues associated with the use of LH_2. A significant concern is related to the loss of containment (LOC), which can arise from accidental scenarios (Ustolin, et al. 2020) or failure components due to hydrogen embrittlement (Campari et al. 2023). LOC may lead to severe consequences, such as boiling liquid expanding vapor explosion (BLEVE) (Ustolin et al. 2020), fireball (Ustolin and Paltrinieri 2020), flash fire (Rigas and Amyotte 2012), vapor cloud explosion (VCE) (Malik et al. 2023), and other phenomena. When LH_2 is released into the environment, the cryogenic liquid partially vaporizes, resulting in a two-phase flow (Jaekel et al. 2012). The amount of liquid fraction that does not flash, may rainout (i.e., a certain number of LH_2 droplets can reach the ground from a release height h), accumulate on the ground, and generate a pool of LH_2. The pool tends to vaporize, forming a cloud of

hydrogen gas, that can disperse and eventually ignite, leading to a flash fire (Holborn et al. 2020). Therefore, the study of rainout and LH_2 pool formation is essential to analyze safety barriers and enable the safe use of hydrogen technologies. Currently, no information is available in the literature regarding the modeling of the LH_2 rainout, except for models implemented in CFD software (Giannissi et al. 2017). In this regard, the existing models (Kim et al. 2022; Gexcon AS 2024) neglect the exact quantification of rainout, assuming that a certain amount of LH_2 will reach the ground and form a pool. This study aims to bridge this knowledge gap by assessing the rainout through an integral model. Concerning this phenomenon, a state-of-the-art model, developed by TNO (2005), is proposed in this study and adapted for liquid hydrogen. This model was developed for liquefied gases, with no mention of substances that are stored at cryogenic temperatures, such as LH_2. Thus, this study analyzed this model to find out its applicability for the rainout of LH_2. The proposed integral model aims to simulate real scenarios of LH_2 pool formation, improving the consequence analyses for hydrogen storage and transport systems.

2. Methodology

The following subsections provide information about the integral model and the steps to use it and perform simulations. The model can be potentially applied to any liquefied substance, e.g., gases that have been compressed to a pressure equal to saturation pressure.

2.1. *DISCHA tool*

DISCHA, developed by the National Center for Scientific Research Demokritos, is a release-modeling tool capable of calculating the stagnation physical properties of different substances, including hydrogen in para and ortho states. DISCHA employs Helmholtz free energy equation of state (EoS) to calculate hydrogen's physical properties, following the formulation provided by (Leachman et al. 2009). The homogeneous equilibrium mixture (HEM) method determines physical properties in the two-phase region, assuming the thermodynamic and hydrodynamic equilibrium between phases. In addition, DISCHA can calculate the steady-state or transient release conditions of substances from storage tanks, including nozzle conditions, for under-expanded releases and transient tank-to-tank transfers. Giving the vapor quality, pressure, and temperature as inputs, DISCHA can determine the fluid density, enthalpy, entropy, void fraction, saturation temperature, saturation pressure, enthalpy of vaporization, internal energy, etc. In this study, DISCHA was used to calculate steady-state or transient release conditions at the nozzle during LH_2 releases. Thus, by computing the internal outlet diameter (D_n), fluid quality (i.e., the ratio of the mass fraction of a two-phase mixture that is in the vapor phase to the total mass) within the tank (ϕ_{tank}), and tank pressure (P_{tank}), DISCHA calculates various exit conditions at the nozzle such as the temperature (T_e), pressure (P_e), velocity (u_e), Mach number (M), mass flux (q_x), mass flow rate (q_e), and fluid quality (ϕ_e). The conditions at the outlet calculated by DISCHA are the starting ground for the application of the model in this study. However, the flow rates of experiments were considered in this study.

2.2. *Tank conditions and case study*

The tank is considered adiabatic since the model focuses on the flashing and rainout of LH_2 and a detailed evaluation of the heat transfer between the tank and the surrounding environment is out of the scope of this study. Additionally, in DISCHA the tank was selected as "homogeneous"; it is therefore assumed that the release occurs under two-phase stagnation conditions. Table 1 summarizes the main specifications of the LH_2 tank.

Table 1. General input of the liquid hydrogen tank.

Parameter	Unit	Value
P_{tank}	MPa	0.6
		0.2
T_{tank}	K	T_{sat} (P_{tank})
V_{tank}	m^3	0.2
D_n	mm	6.0
		12.0
		24.0
ϕ_{tank}	-	0.0
		0.2

Simulations of LH_2 releases were carried out considering the experimental data for the horizontal releases of the PRESHLY project (Lyons et al. 2020). The same nozzle diameters (D_n), tank pressure (P_{tank}), flow rate ($q_{S,e}$), and release height ($h_{release}$) were used for the rainout simulations. These data are presented in Table 2, which summarizes the testing conditions of four experiments. The pressure drops obtained in the experiments from control valves, vacuum hose, flow meter, release globe valve, and other fittings, are neglected. Thus, considering also that the tank is assumed adiabatic, the nozzle conditions are expected to be conservative since the fluid at the nozzle will be in a state with a higher quality factor.

Table 2. Data from PRESHLY project experiments.

Test No.	P_{tank} $[MPa]$	D_n $[mm]$	$q_{S,e}$ $\left[\frac{kg}{s}\right]$	$h_{release}$ $[m]$
1	0.600	6.000	0.095	0.500
2	0.200	12.000	0.105	0.500
3	0.600	12.000	0.265	0.500
4	0.200	24.000	0.140	0.500

In addition, this study considers a conservative case with a fluid quality of $\phi_{tank} = 0$, and another case with $\phi_{tank} = 0.2$ to evaluate a less conservative scenario.

2.3. Flashing and rainout model

The model to calculate the jet conditions after flashing and rainout is based on the equations reported in the Yellow Book (TNO 2005).

2.3.1. *Calculation of the conditions in the jet after flashing*

This subsection provides a guide to estimate the flash fraction, jet velocity, radius, and density of the flashed jet. To describe the depressurization of liquid hydrogen released, the following quantities must be given as inputs: pressure at the outlet P_e, temperature at the outlet T_e [K], cross-section of the hole A_e [m^2], total mass flow rate $q_{S,e}$ [kg/s], and vapor mass fraction (or "fluid quality") at the outlet ϕ_e [-]. As the fluid flows from higher pressure (i.e., the storage tank) to lower pressure environments (i.e., the ambient air), a depressurization and a consequent flash of the liquid phase occur. First, the velocity of the jet must be calculated through the momentum and mass conservation (Eq. (1)):

$$u_f = \frac{(P_e - P_{atm}) \cdot A_e}{q_{S,e}} + u_e \quad (1)$$

where u_e [m/s] is the flow velocity at the outlet. The quality after flashing can be calculated from the conservation of total energy (Eq. (2)):

$$\phi_{m,f} = 1 - \frac{H_{vf} - H_{ve} + (1 - \Phi_e) \cdot L_{ve} + 0.5 \cdot \left(u_f^2 - u_e^2\right)}{L_{vf}} \quad (2)$$

where H_{vf} [J/kg] is the enthalpy of the vapor at boiling temperature and atmospheric pressure; H_{ve} [J/kg] is the enthalpy of the vapor at the exit temperature; L_{ve} [J/kg] is the latent heat of evaporation at exit conditions; L_{vf} [J/kg] is the latent heat of evaporation after flashing, at atmospheric pressure. Then, the jet cross-section A_f [m^2] and jet radius b_f [m] can be obtained as per Eq. (3) and Eq. (4):

$$A_f = \rho_e \cdot u_e \cdot \frac{A_e}{\rho_f \cdot u_f} \quad (3)$$

$$b_f = \sqrt{\frac{A_f}{\pi}} \quad (4)$$

2.3.2. *Calculation of the droplet diameter after flashing*

This model can calculate only one dimension for all drops. The droplet size can be calculated as per Eq. (5a) and (5b):

$$d_{d,f} = 3.78 \cdot b_f \cdot \sqrt{1 + 3 \cdot \frac{\left(2 \cdot b_f \cdot u_f^2 \cdot \frac{\rho_{Lf}}{\sigma_s}\right)^{0.5}}{2 \cdot b_f \cdot \frac{u_f}{v_L}}}$$

$$\text{if } 2 \cdot b_f \cdot u_f^2 \cdot \frac{\rho_{Lf}}{\sigma_s} < \left(2 \cdot b_f \cdot \frac{u_f}{v_L}\right)^{-0.45} \cdot 10^6 \text{ and } T_e < 1.11 \cdot T_B \quad (5a)$$

Otherwise:

$$d_{d,f} = C_{ds} \cdot \frac{\sigma_s}{u_f{}^2 \cdot \rho_a} \quad (5b)$$

where ρ_a [kg/m^3] is the density of the air; C_{ds} is a constant, which varies from 10 to 20; T_B [K] is the normal boiling temperature; ρ_{Lf} [kg/m^3] is the liquid hydrogen density after flashing; σ_s [N/m] is the surface tension between the liquid and the vapor; v_L [m^2/s] is the kinematic viscosity of liquid hydrogen after flashing.

2.3.3. *Droplet evaporation*

In this section, the evolution of the droplet size due to evaporation is assumed to be the same for all droplets. The relative velocity of the droplet in the air, which corresponds to the fall velocity of the droplet, can be expressed as per Eq. (6):

$$u_d = \frac{\rho_{Lf} \cdot g \cdot d_d^2}{18 \cdot v_a \cdot \rho_a} \quad (6)$$

where ρ_{Lf} [kg/m^3] is the density of the droplet at the boiling temperature and v_a [m^2/s] is the kinematic viscosity of the ambient air.

After flashing, the liquid hydrogen droplets and aerosol may fall to the ground forming a pool or vaporize before reaching the ground. To consider the evaporation of the droplets' surface, the coefficient k_B [m^2/s] is defined as per Eq. (7):

$$k_B = \frac{4 \cdot \mu_i \cdot D \cdot P_a}{\rho_{Lf} \cdot R \cdot T_a} \cdot \ln\left(1 + \frac{P_s(T_d)}{P_a}\right) \quad (7)$$

where μ_i [g/mol] is the molar weight of liquid hydrogen or any other chemicals released; R [J/mol·K] is the universal gas constant; T_a [K] is the ambient temperature; $P_s(T_d)$ [MPa] is the saturation pressure of the released chemical at the droplet temperature T_d. This study adopts an updated formula for Eq. (7), where the original minus sign within the logarithm argument has been replaced with a plus sign. As a result, the formula can also work for saturation pressures higher than the ambient pressure. However, this needs to be validated and is purely a mathematical adjustment to apply the equation.

The droplet temperature is calculated through Eq. (8):

$$T_d = T_a - \frac{L_{v,d} \cdot k_B \cdot \rho_{Lf} \cdot \left(1 + 0.28 \cdot Re_d^{\frac{1}{2}} \cdot S_c^{\frac{1}{3}}\right)}{4 \cdot \lambda \cdot \left(1 + 0.28 \cdot Re_d^{\frac{1}{2}} \cdot P_r^{\frac{1}{3}}\right)} \quad (8)$$

where Re_d is the Reynolds number, S_c is the Schmidt number, P_r is the Prandtl number, and λ is the thermal conductivity of the air. The Reynolds number must be calculated using the relative velocity of the droplet. TNO (2005) does not point out the meaning of the parameter $L_{v,d}$. Given the previous definition of the latent heat of evaporation in Eq. (2), in this study it is assumed that the aforementioned parameter is the latent heat of evaporation calculated at the droplet temperature T_d.

However, in Eq. (7), the parameter k_B depends on $P_s(T_d)$, i.e., the saturation pressure at the droplet temperature T_d. On the other hand, in Eq. (8) the droplet temperature T_d depends on the parameter k_B, which leads to an equation with two unknowns. This problem has been solved iteratively, assuming an initial value of T_d equal to the temperature of liquid hydrogen within the tank and iterating until convergence with a 1% error criterion. Simultaneously, the code retrieves the thermodynamic properties from the CoolProp package (Bell et al. 2014). Specifically, for liquid hydrogen, the iteration proposed always predicts that the droplet temperature reaches a value greater than the critical temperature of LH_2, causing the interruption of the iteration for the calculation of k_B and T_D. This suggests that when the droplet is fully evaporated, the iteration cannot proceed further, and it is not possible to calculate T_D. However, subsection 3.2 explains why this may occur. In this study, to better analyze the phenomenon, when the iteration could not proceed further, a $P_s(T_d)$ corresponding to the critical temperature of LH_2 is considered. Once T_d is calculated, the maximum diameter of a liquid hydrogen droplet that will rain out on the ground can be approximated through Eq. (9):

$$d_M = 2 \cdot \left\{ \frac{9 \cdot \rho_a \cdot v_a \cdot k_B \cdot h_s}{2 \cdot \rho_{Lf} \cdot g} \cdot \left[1 - 0.204 \cdot S_c^{\frac{1}{3}} \cdot \left(\frac{\rho_{Lf} \cdot g}{18 \cdot \rho_a \cdot {v_a}^2} \right)^{\frac{1}{2}} \left(\frac{72 \cdot \rho_a \cdot v_a \cdot k_B \cdot h_s}{\rho_{Lf} \cdot g} \right)^{\frac{3}{8}} \right]^{-1} \right\}^{\frac{1}{4}} \quad (9)$$

where h_s is the release height. Rainout occurs if the droplet size after flashing $d_{d,f}$ is larger than the maximum rainout droplet d_M. Notably, the methodology is applicable only if $Re_d < 4$, calculated considering d_M. If $Re_d > 4$, the evolution of the droplet diameter $d_d(t)$, considering the evaporation of the droplet while falling on the ground, needs to be evaluated through Eq. (10):

$$\frac{d}{dt} d_d = -\frac{k_B}{d_d} \cdot \left(1 + 0.28 \cdot {Re_d}^{\frac{1}{2}} \cdot S_c^{\frac{1}{3}}\right) \quad (10)$$

This integration must be performed until the droplet reaches the ground or evaporates from a starting height h_s. However, the reduction of the droplet diameter over time causes a variation of the relative velocity u_d calculated with Eq. (6). Considering a horizontal release without initial velocity in the y-direction, the evolution of the height at which the drop is located can be studied with the following integration (Eq. (11)):

$$0 = h(t_0) = h_s - \int_0^{t_0} u_d \, dt \quad (11)$$

Eq. (10) and Eq. (11) must be solved simultaneously until the droplet reaches the ground or evaporates completely. The equations were solved by updating Re_d at each time step as the drop height and relative velocity u_d changed over time.

2.3.4. *Rainout on the ground*

The net vapor mass released by the jet is calculated considering the initial vapor already present in the jet after flashing and the vapor generated from the evaporation of the droplets during their fall:

$$q_V = q_{S,e} \cdot \phi_{m,f} + \left(1 - \phi_{m,f}\right) \cdot \left(1 - \left[\frac{d_0}{d_d}\right]^3\right) \cdot q_{S,e} \quad (12)$$

where d_0 is the final droplet diameter when they reach the ground. Eq. (12) implies that the liquid that reaches the ground does not contribute to the liquid that evaporates and does not mix with the vapor in the jet. Thus, the amount of liquid reaching the ground is defined by the following equation:

$$q_L = q_{S,e} - q_V \quad (13)$$

where q_L [kg/s] is the total mass flow rate of liquid hydrogen reaching the ground.

When the droplets reach the ground, they are subjected to heat conduction, radiation, and convection, leading to a rapid pool evaporation (Middha et al. 2011). The available studies on pool evolution do not consider the flashing effect of the fluid and the droplet evaporation while falling on the ground, leading to incorrect and overestimated results. However, by considering $q_{S,l}$ a real pool spreading and evolution scenario can be studied.

3. Results and discussion

This section discusses the results in subsection 3.1, while section 3.2 is dedicated to the model limitations.

3.1. *Rainout simulations*

Rainout simulations were performed using the experimental data of the PRESHLY project, summarized in Table 2. These experiments were replicated twice, considering a fluid quality factor of $\phi_{tank} = 0$ and $\phi_{tank} = 0.2$. Thus, Table 3 presents the simulation results based on the data from the PRESHLY experiments for tests No. 1.1 to No. 4.2, while tests A and B represent scenarios that are not included in the PRESHLY experiments. According to the PRESHLY tests, these simulations did not predict any rainout phenomena. However, some peculiarities emerged from the analysis. On the one hand, for higher pressures at the nozzle, $\phi_{m,f}$ increases significantly compared to ϕ_e. On the other hand, for pressures close to ambient pressure, $\phi_{m,f}$ decreases compared to ϕ_e, indicating a much less pronounced flashing phenomenon. This phenomenon might be explained because, for saturation temperatures above approximately 25 K, the enthalpy of vaporization L_{vf} is significantly higher than L_{ve}. In contrast, at lower pressures, this difference is less pronounced. Thus, these results suggest that rainout experiments should be designed so that the pressure at the nozzle corresponds to a saturation temperature below 25 K, which would reduce the flashing, i.e., the liquid hydrogen evaporation. Nevertheless, it is important to ensure that the pressure at the nozzle is not significantly impacted by pressure drops along the pipeline, as friction-induced heat might trigger phase changes of LH_2. Moreover, considering a P_{tank}= 0.6 MPa, as ϕ_e increases, the diameter of the liquid hydrogen droplet $d_{d,f}$ decreases, reducing the likelihood of a rainout event. Conversely, considering a $P_{tank} =$ 0.2 MPa, as ϕ_e increases, the droplet diameter increases. This occurs since, considering a $\phi_{tank} =$ 0.2, ϕ_e increases, and the pressure calculated at the nozzle P_e is lower than that obtained with a $\phi_{tank} =$ 0. Thus, the pressure at the nozzle appears to be one of the key parameters for rainout events. If the pressure decreases, the relative velocity u_f decreases as well, and the droplet diameter d_d consequently increases, thereby enhancing the potential for rainout. Furthermore, another key parameter is the flow velocity at the outlet u_e, which is inversely proportional to the outlet area A_e. Indeed, increasing the outlet section and keeping the same flow rate while considering a P_e almost equal to the ambient pressure, rainout occurs, as illustrated in tests A and B. In these tests, considering a P_e nearly the same as the ambient pressure, this time escalating the quality factor ϕ_e, the droplet diameter decreased. This occurs

because the pressure at the nozzle is already close to the ambient pressure. Thus, an increase in ϕ_e cannot cause a further reduction of P_e, pointing out that for the same nozzle pressure, the quality factor ϕ_e is another key parameter for rainout events. These results indicate that fluid quality at the nozzle is a key parameter in experiments, that needs to be monitored both along the pipeline and at the nozzle to investigate the rainout phenomenon. The results show that the pressure at the nozzle must be higher than the ambient pressure to avoid rainout, and the higher the fluid quality, the lower the rainout. Figure 1 illustrates the influence of changing ϕ_e on the liquid hydrogen flow rate that reaches the ground, considering a release height of h = 0.5 m and the thermodynamic parameters from test A.

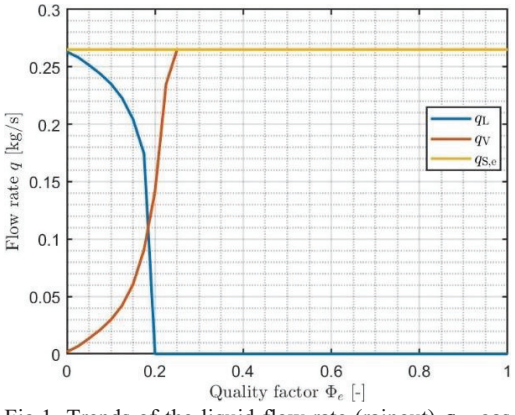

Fig.1. Trends of the liquid flow rate (rainout) q_L, gas flow rate q_V, and released flow rate $q_{S,e}$ as a function of the fluid quality at the outlet.

As the quality factor increases, the flow rate of hydrogen gas released to the environment (q_V) increases, while the amount of liquid hydrogen that reaches the ground (q_L) decreases. Thus, these results prove once again that fluid quality is a crucial parameter, and, for high fluid quality, rainout is unlikely to occur. These results are not only useful for the design of LH_2 release experiments but also to improve the safety of hydrogen systems in industrial settings. For instance, maintaining the pressure at the nozzle higher than the atmospheric one can reduce the risk of rainout phenomena, avoiding the dispersion of liquid hydrogen on the ground or other materials.

3.2 *Model limitations*

The model proposed considers the effect of the ambient temperature on the individual droplet. Nevertheless, the heat capacity of the entire hydrogen jet, i.e., the heat capacity of the gas and all the liquid droplets, should be considered. In addition, a droplet located in the middle of the jet may not be subjected to the ambient temperature but rather to the temperature of the surrounding hydrogen gas (Sprittles 2024; Gottfried et al. 1966). Therefore, during the iteration proposed in subsection 2.3.3, when T_D reaches a value higher than the critical temperature, the maximum saturation pressure of liquid hydrogen is used to calculate k_B. Considering the thermal capacity of the jet and the proximity of hydrogen droplets, it is expected that the results will be more conservative and the diameter of liquid hydrogen droplets that can reach the ground will increase.

Table 3. Rainout simulations considering a height release of 0.5 m.

Test No.	P_{tank} $[MPa]$	P_e $[MPa]$	T_e $[K]$	ϕ_e $[-]$	D_n $[mm]$	$q_{S,e}$ $\left[\frac{kg}{s}\right]$	$\phi_{m,f}$ $[-]$	$d_{d,f}$ $[mm]$	q_L $\left[\frac{kg}{s}\right]$
1.1	0.600	0.400	26.084	0.078	6.000	0.095	0.162	$0.654 \cdot 10^{-3}$	0.000
1.2	0.600	0.363	25.605	0.250	6.000	0.095	0.283	$0.254 \cdot 10^{-3}$	0.000
2.1	0.200	0.146	21.682	0.028	12.000	0.105	0.039	$0.419 \cdot 10^{-3}$	0.000
2.2	0.200	0.119	20.943	0.221	12.000	0.105	0.220	$0.914 \cdot 10^{-3}$	0.000
3.1	0.600	0.400	26.084	0.078	12.000	0.265	0.153	$0.606 \cdot 10^{-3}$	0.000
3.2	0.600	0.363	25.605	0.250	12.000	0.265	0.276	$0.325 \cdot 10^{-3}$	0.000
4.1	0.200	0.146	21.682	0.028	24.000	0.140	0.018	$0.101 \cdot 10^{-3}$	0.000
4.2	0.200	0.119	20.943	0.221	24.000	0.140	0.216	$2.126 \cdot 10^{-3}$	0.000
A	$\approx P_a$	$\approx P_a$	20.365	0.000	100.000	0.265	0.000	3.544	0.263
B	$\approx P_a$	$\approx P_a$	20.365	0.152	100.000	0.265	0.152	1.338	0.202

4. Conclusion

This study is a preliminary approach toward the evaluation of real scenarios of LH_2 pool formation. Although the model can be applied to different liquefied gases, it is validated for liquid hydrogen releases only. The integral model estimates the size of LH_2 droplets after a release, their evaporation rate, and the amount of liquid reaching the ground. The results of the simulations were compared with experimental data from the PRESHLY project, reiterating that rainout does not occur under the simulated operating conditions. In addition, the simulations showed that rainout is affected by key parameters such as pressure and fluid quality at the nozzle, and jet velocity.

The analysis showed that for pressures significantly higher than atmospheric pressure and high fluid quality, the rainout is dramatically reduced, while for lower pressures and larger release sections, the phenomenon becomes more likely. However, the model revealed some limitations related to the estimation of the heat capacity of the entire hydrogen jet and the interaction of the droplets with the surrounding environment. The methodology appears not conservative when adopted for cryogenic fluids. Despite these limitations, the developed model provides useful insights for safety analysis in LH_2 storage and transport. Future studies will include refinement of droplet evaporation modeling and a more detailed analysis of the thermodynamic interaction between the jet and the environment.

5. Acknowledgements

This work was carried out under the activities of HYDROGENi (RCN, Project No. 333118), the Norwegian research and innovation centre for hydrogen and ammonia financed by the Norwegian Research Council's Centres for Environment-friendly Energy Research (FME) program and coordinated by SINTEF. Furthermore, this work was undertaken as part of the ELVHYS project No. 101101381 supported by the Clean Hydrogen Partnership and its members and the European Union. UK participants in Horizon Europe Project ELVHYS are supported by UKRI grant numbers 10063519 (University of Ulster) and 10070592 (Health and Safety Executive). Funded by the European Union. Views and opinions expressed are however those of the author(s) only and do not necessarily reflect those of the European Union or Clean Hydrogen JU. Neither the European Union nor the granting authority can be held responsible for them.

References

Aziz, Muhammad. 2021. "Liquid Hydrogen: A Review on Liquefaction, Storage, Transportation, and Safety." *Energies* 14 (18). https://doi.org/10.3390/en14185917.

Bell, Ian H., Jorrit Wronski, Sylvain Quoilin, and Vincent Lemort. 2014. "Pure and Pseudo-Pure Fluid Thermophysical Property Evaluation and the Open-Source Thermophysical Property Library CoolProp." *Industrial & Engineering Chemistry Research* 53:2498–2508. https://doi.org/doi:10.1021/ie4033999.

Campari, Alessandro, Federico Ustolin, Antonio Alvaro, and Nicola Paltrinieri. 2023. "A Review on Hydrogen Embrittlement and Risk-Based Inspection of Hydrogen Technologies." *International Journal of Hydrogen Energy* 48 (90): 35316–46. https://doi.org/10.1016/j.ijhydene.2023.05.293.

Gexcon AS. 2024. "FLACS-CFD V24.1 User's Manual."

Giannissi, Stella G.;, Alexandros G.; Venetsanos, Elena; Vyazmina, Simon; Jallais, Simon Coldrick, and Kieran; Lyons. 2021. "CFD Simulations of Large Scale LH2 Dispersion in Open Environment," 1–11.

Gottfried, Byron S., C. J. Lee, and Kenneth J. Bell. 1966. "The Leidenfrost Phenomenon: Film Boiling of Liquid Droplets on a Flat Plate." *International Journal of Heat and Mass Transfer* 9 (11): 1167–88. https://doi.org/10.1016/0017-9310(66)90112-8.

Holborn, Paul G., Claire M. Benson, and James M. Ingram. 2020. "Modelling Hazardous Distances for Large-Scale Liquid Hydrogen Pool Releases." *International Journal of Hydrogen Energy* 45 (43): 23851–71. https://doi.org/10.1016/j.ijhydene.2020.06.131.

Jaekel, Christian, Karl Verfondern, Stephan Kelm, Wilfried Jahn, and Hans Josef Allelein. 2012. "3D Modeling of the Different Boiling Regimes during Spill and Spreading of Liquid Hydrogen." *Energy Procedia* 29:244–53. https://doi.org/10.1016/j.egypro.2012.09.030.

Jin, Tao, Mengxi Wu, Yuanliang Liu, Gang Lei, Hong Chen, and Yuqi Lan. 2017. "CFD Modeling and Analysis of the Influence Factors of Liquid Hydrogen Spills in Open Environment." *International Journal of Hydrogen Energy* 42 (1): 732–39. https://doi.org/10.1016/j.ijhydene.2016.10.162.

Juangsa, Firman Bagja, Lukman Adi Prananto, Zahrul Mufrodi, Arief Budiman, Takuya Oda, and Muhammad Aziz. 2018. "Highly Energy-Efficient Combination of Dehydrogenation of Methylcyclohexane and Hydrogen-Based Power Generation." *Applied Energy* 226

(January): 31–38. https://doi.org/10.1016/j.apenergy.2018.05.110.

Kim, Soohyeon, Minkyung Lee, Junghwan Kim, and Jaehun Lee. 2022. "Diffusion Range and Pool Formation in the Leakage of Liquid Hydrogen Storage Tank Using CFD Tools." *Applied Chemistry for Engineering* 33 (6): 653–60. https://doi.org/10.14478/ace.2022.1115.

Leachman, Jacob W., Richard T. Jacobsen, S. G. Penoncello, and Eric W. Lemmon. 2009. "Fundamental Equations of State for Parahydrogen, Normal Hydrogen, and Orthohydrogen." *Journal of Physical and Chemical Reference Data* 38 (3): 721–48. https://doi.org/10.1063/1.3160306.

Lyons, Kieran, Simon Coldrick, and Graham Atkinson. 2020. "Summary of Experiment Series E3.5 (Rainout) Results." Vol. 5.

Malik, Darren R., W. B. Lowry, E. Vivanco, and J. K. Thomas. 2023. "Very Lean Hydrogen Vapor Cloud Explosion Testing." *Process Safety Progress* 42 (2): 242–51. https://doi.org/10.1002/prs.12459.

Middha, Prankul, Mathieu Ichard, and Bjørn J. Arntzen. 2011. "Validation of CFD Modelling of LH2 Spread and Evaporation against Large-Scale Spill Experiments." *International Journal of Hydrogen Energy* 36 (3): 2620–27. https://doi.org/10.1016/j.ijhydene.2010.03.122.

Rigas, Fotis, and Paul Amyotte. 2012. *Hydrogen Safety*. Green chemistry and chemical engineering.

Semieniuk, Gregor, Lance Taylor, Armon Rezai, and Duncan K. Foley. 2021. "Plausible Energy Demand Patterns in a Growing Global Economy with Climate Policy." *Nature Climate Change* 11 (4): 313–18. https://doi.org/10.1038/s41558-020-00975-7.

Sprittles, James E. 2024. "Gas Microfilms in Droplet Dynamics: When Do Drops Bounce?" *Annual Review of Fluid Mechanics* 56:91–118. https://doi.org/10.1146/annurev-fluid-121021-021121.

TNO. 2005. *Yellow Book - Methods for the Calculation of Physical Effects Due to Releases of Hazardous Materials (Liquids and Gases)*. Edited by R.A.P.M. Weterings C.J.H. van den BOSCH. Third edit. The Hague.

Ustolin, Federico, and Nicola Paltrinieri. 2020. "Hydrogen Fireball Consequence Analysis." *Chemical Engineering Transactions* 82 (January): 211–16. https://doi.org/10.3303/CET2082036.

Ustolin, Federico, Nicola Paltrinieri, and Filippo Berto. 2020. "Loss of Integrity of Hydrogen Technologies : A Critical Review." *International Journal of Hydrogen Energy* 45 (43): 23809–40. https://doi.org/10.1016/j.ijhydene.2020.06.021.

Ustolin, Federico, Ernesto Salzano, Gabriele Landucci, and Nicola Paltrinieri. 2020. "Modelling Liquid Hydrogen Bleves: A Comparative Assessment with Hydrocarbon Fuels." *Proceedings of the 30th European Safety and Reliability Conference and the 15th Probabilistic Safety Assessment and Management Conference*, no. May 2021, 1876–83. https://doi.org/10.3850/978-981-14-8593-0_3982-cd.